

Fourier-Rectangular Function Analysis of Spatiotemporal Structure of Bursting Phenomenon in a Cylindrical Plasma

Daiki NISHIMURA, Akihide FUJISAWA¹⁾, Yoshihiko NAGASHIMA¹⁾, Chanhoo MOON¹⁾, Kotaro YAMASAKI²⁾, Taiki KOBAYASHI and Shigeru INAGAKI¹⁾

*Interdisciplinary Graduate School of Engineering Sciences, Kyushu University,
6-1 Kasuga-koen, Kasuga, Fukuoka 816-8580, Japan*

¹⁾*Research Institute for Applied Mechanics, Kyushu University, 6-1 Kasuga-koen, Kasuga, Fukuoka 816-8580, Japan*

²⁾*Department of Mechanical Engineering, Graduate School of Engineering, Hiroshima University,
Higashihiroshima, Hiroshima 739-8527, Japan*

(Received 7 April 2021 / Accepted 16 April 2021)

The tomography measurement, with a help of a newly developed analysis called Fourier-rectangular function (FRF) transform, reveals the properties of the bursting phenomenon occurring at the lower operational boundary of the filling pressure in a cylindrical plasma produced with a helicon source. The analysis provided a clear difference in the spatiotemporal structure between the bursting and quiescent states in the phenomenon.

© 2021 The Japan Society of Plasma Science and Nuclear Fusion Research

Keywords: tomography, fluctuation, linear magnetized plasma, plasma emission, asymmetry

DOI: 10.1585/pfr.16.1201075

The research on two-dimensional plasma structure [1] has started in Plasma Assembly for Nonlinear Turbulence Analysis (PANTA) using tomography systems [2, 3]. The measurement has developed advanced tools to analyze 2D-tomography image, such as Fourier-rectangular function (FRF) transform [4] and its polarization analysis [5]. The PANTA device produces a cylindrical plasma, whose diameter is 0.1 m along a straight magnetic field. In the operation boundary at the lower filling pressure at 0.6 mTorr with the heating power of 3 kW and magnetic field of 0.09 T, the Argon plasmas are found to show intermittent bursts rising from a quiescent state. The tomography measurement identifies clear difference between the quiescent and bursting phases in its spatiotemporal properties with a help of FRF analysis

In the tomography, the obtained line-integrated data are reconstructed to local emission profile with Maximum Likelihood Expectation Maximization (MLEM). The MLEM profile is expanded in polar coordinate using FRF transform in the following form,

$$\varepsilon(r_n, \theta) \simeq \sum_{n=1}^{N_r} \left[a_{0n} \frac{R(r_n)}{\sqrt{2}} + \sum_{m=1}^M R(r_n) [a_{mn} \cos(m\theta) + b_{mn} \sin(m\theta)] \right], \quad (1)$$

where N_r is the number of rectangular functions used for expansion, and m is an azimuthal mode number. The function, $R(r_n)$, has a finite value in a radial band indicated by n . By making complex variables, $c_{mn}(t) = a_{mn}(t) + ib_{mn}(t)$ the local power and the polarization property of a mode

are evaluated from $P_{mn}(t) = |c_{mn}(t)|^2$ and its argument, respectively. Moreover, combinations of their Fourier transformed coefficients, $\hat{c}_{mn,R}(f) = \hat{a}_{mn}(f) + i\hat{b}_{mn}(f)$ and $\hat{c}_{mn,L}(f) = \hat{a}_{mn}^*(f) + i\hat{b}_{mn}^*(f)$, represent the components rotating in the electron and ion diamagnetic direction, respectively, where $\hat{a}_{mn}(f)$ and $\hat{b}_{mn}(f)$ are the Fourier coefficients with $\hat{a}_{mn}^*(f)$ and $\hat{b}_{mn}^*(f)$ being their conjugates. The coefficients can resolve the polarization properties [5]. The method is simply extended to the case of Morlet wavelet transform due to its correspondence with Fourier transform.

The measurement of the entire plasma cross-section was performed in every 1 μ s for the period from 200 to 500 ms where the plasma property is regarded as being unchanged for the entire discharge duration of 600 ms. Figure 1 shows the overall plasma characteristics. The emission is divided into two parts as $\varepsilon(r, t) = \bar{\varepsilon}(r, t) + \tilde{\varepsilon}(r, t)$, where $\bar{\varepsilon}(r, t)$ and $\tilde{\varepsilon}(r, t)$ are the slowly developing and the fluctuating part, respectively; $\bar{\varepsilon}(r, t) = \int_{-T/2}^{T/2} \varepsilon(t) dt / T$ with $T = 5$ ms for the slowly developing part. The total emission defined as $\varepsilon_{tot}(t) = \sum_n \varepsilon(r_n, t) \Delta S_n$ with ΔS_n being the area of n -th radial band. The total fluctuation power, $\tilde{P}_{tot}(t) = \int \tilde{P}(f, t) df$, with $\tilde{P}(f, t)$ is the power density, and the fluctuation amplitude is $\tilde{A}_{tot}(t) = \sqrt{\tilde{P}_{tot}(t)}$. In the calculation, the Morlet wavelet [6] is used here to resolve temporal behavior of the plasma.

The temporal evolution in Fig. 1 (a) suggests that a correlation in rises and falls exists of these two quantities, $\varepsilon_{tot}(t)$ and $\tilde{A}_{tot}(t)$. The total emission fluctuates at random due to its Gaussian property of their PDF, while the fluctuation amplitude implies two distinguished states;

author's e-mail: nishimura.daiki@riam.kyushu-u.ac.jp

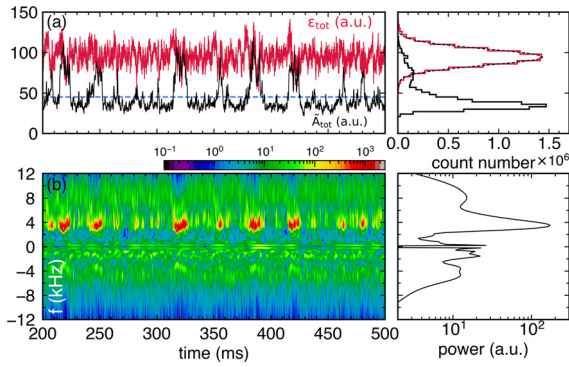


Fig. 1 (a) Temporal evolutions of total emission (red line) and fluctuation amplitude (black line) and their PDFs with a Gaussian for reference. The blue line shows the average of fluctuation amplitude. (b) The temporal evolution of the Morlet wavelet spectrum, and its temporally-average. The positive and negative frequency represent the component rotating in the electron and ion diamagnetic direction, respectively.

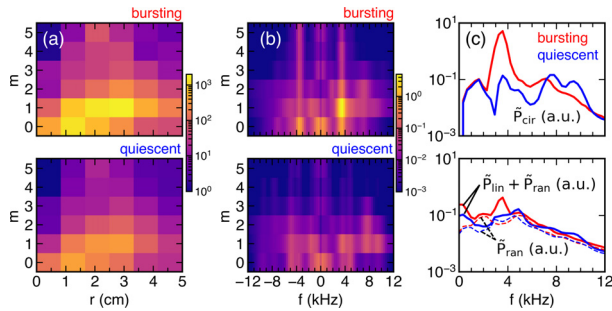


Fig. 2 The FRF properties of bursting and quiescent states. (a) FRF spectra, radial profile of the intensities of each azimuthal mode number. (b) FRF dispersion relation, and (c) the powers of polarizations for the two states. The dashed lines represent the random polarization powers.

the quiescent state in which the plasma stays for most of the discharge period, and the other long tail region with a small peak corresponding to the bursting state. The temporal evolution of the wavelet spectrum in Fig. 1 (b) indicates that the most dominant mode in the bursting phase is at the frequency at $f \sim 3.7$ kHz, which rotates in the electron diamagnetic direction. The bursting phase is found to last for significantly longer time than a cycle of the mode at $f \sim 3.7$ kHz. Thus, the intermittent phenomenon can be regarded as transitions from a quiescent state to a bursting one.

Figure 2 shows the FRF spectra averaged over the entire period of the analysis, and the dispersion relations for the two states with their polarization characteristics. The FRF spectra, shown in Fig. 2 (a), indicates that the clear increase, particularly in the $m = 1$ mode power, which is located approximately $r \sim 3$ cm. The FRF dispersion relations, shown in Fig. 2 (b), obtained from the Fourier

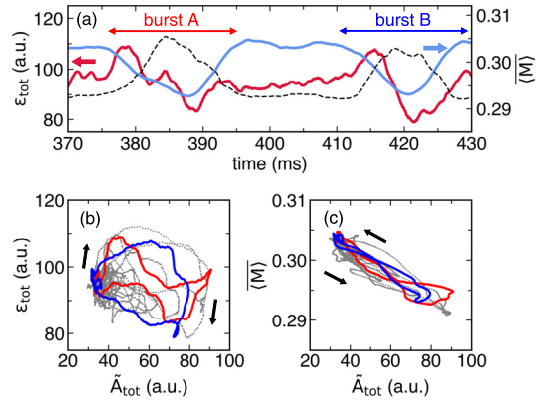


Fig. 3 A detailed view of (a) temporal evolutions of total fluctuations amplitude, $\tilde{A}_{tot}(t)$ and the background m-number, $\langle M \rangle(t)$ with the total emission, $\varepsilon_{tot}(t)$. (b) Lissajous diagrams of $\tilde{A}_{tot}(t)$ and $\varepsilon_{tot}(t)$, and (c) that of $\tilde{A}_{tot}(t)$ and $\langle M \rangle(t)$. The red and blue lines are for burst A and burst B, respectively, with the dotted lines for the entire period of the analysis.

transform of FRF coefficients, indicate unambiguously that the mode at $f \sim 3.7$ kHz, which has $m = 1$ mode structure, should be significantly dominant in the bursting state. Moreover, the polarization properties of fluctuations are analyzed, where the powers of circular, linear and random polarization are denoted as \tilde{P}_{cir} , \tilde{P}_{lin} and \tilde{P}_{ran} [5]. The bursting state is dominated by the circular polarized component of the $m = 1$ mode, as shown in Fig. 2 (c). For further comparison, the spatially-averaged background m-number defined as follows

$$\langle M \rangle = \frac{1}{T} \int_{-T/2}^{T/2} \frac{\sum_m \sum_n m \cdot P_{S,mn}(t)}{\sum_m \sum_n P_{S,mn}(t)} dt, \quad (2)$$

where $P_{S,mn}(t)$ is the slowly developing part of the FRF coefficient power. The background m-number for bursting and quiescent state are 0.296 and 0.303, respectively. Thus, the bursting mode should be characterized by the recovery of symmetry, as is indicated in the m-number closer to zero.

The causal relation is examined for the transition between the two states. Figure 3 shows the detailed comparison of temporal evolutions, which provides 1) the increase in the total emission could be the trigger to the bursting behavior, 2) the total emission decreases with the bursts of the fluctuations, 3) the rises and falls of the total fluctuation powers are well anti-correlated with those of the background m-number with the average period of $T = 5$ ms. The findings are also confirmed in the Lissajous diagrams.

Finally, the FRF and its polarization analysis shows that the bursting state is characterized by an increase in circularly polarized $m = 1$ mode, which could be triggered by the rise of total emission, and that the burst is accompanied with the decreasing the background m-number, which

means the recovery of symmetry in the background emission profile.

This work is supported by JSPS KAKENHI (Grant Numbers. JP17H06089, JP19K23426, JP20K14443 and JP21K13898) and also by the NIFS Collaboration Research program (NIFS17KOCH002 & 21KLPH050).

- [1] G.S. Yun *et al.*, Phys. Rev. Lett. **107**, 045004 (2011).
- [2] A. Fujisawa *et al.*, Plasma Phys. Control. Fusion **58**, 025005 (2016).
- [3] C. Moon *et al.*, Sci. Rep. **11**, 3720 (2021).
- [4] K. Yamasaki *et al.*, J. Appl. Phys. **126**, 043304 (2019).
- [5] D. Nishimura *et al.*, J. Appl. Phys. **129**, 093301 (2021).
- [6] J. Morlet *et al.*, Geophysics **47**, 2 (1982).